General Disclaimer

One or more of the Following Statements may affect this Document

- This document has been reproduced from the best copy furnished by the organizational source. It is being released in the interest of making available as much information as possible.

- This document may contain data, which exceeds the sheet parameters. It was furnished in this condition by the organizational source and is the best copy available.

- This document may contain tone-on-tone or color graphs, charts and/or pictures, which have been reproduced in black and white.

- This document is paginated as submitted by the original source.

- Portions of this document are not fully legible due to the historical nature of some of the material. However, it is the best reproduction available from the original submission.

NASA Technical Memorandum 83028
AIAA-83-0337

Small Gas Turbine Combustor Study – Combustor Liner Evaluation

(NASA-TM-83028) SMALL GAS TURBINE COMBUSTOR   N83-18725
STUDY: COMBUSTOR LINER EVALUATION (NASA)
20 p HC A02/MF A01   CSCL 21E
                                                Unclas
                                        G3/07 02419

Carl T. Norgren and Stephen M. Riddlebaugh
Lewis Research Center
Cleveland, Ohio

NASA

SMALL GAS TURBINE COMBUSTOR STUDY -
COMBUSTOR LINER EVALUATION

Carl T. Norgren and Stephen M. Riddlebaugh

National Aeronautics and Space Administration
Lewis Research Center
Cleveland, Ohio

E-1463

Abstract

A reverse flow combustor liner constructed of
Lamilloy (a multilaminate transpiration type mate-
rial) is compared both analytically and experi-
mentally with a conventional splash film-cooled
design with the same combustor configuration. Com-
parison of selected critical combustor panels indi-
cated that it was possible to maintain the liner
temperature similar between the two configurations
using 50 percent less coolant for the Lamilloy as
compared with the reference film-cooled combustor.
Additional benefits indicated improvement in outlet
temperature distribution and NO_x emission level.

Introduction

As part of the overall continuing research
effort at the NASA Lewis Research Center to improve
performance, emissions and reliability of the com-
ponents of a gas-turbine engine an evaluation of
combustor liner cooling techniques was undertaken.
Small gas-turbine engines encompass a rather broad
power range from a hundred shaft horsepower or less
to well into the thousands of horsepower and in-
clude such diverse applications as helicopters,
general aviation, commuter-craft, as well as ord-
nance. Potential for extending the mission capa-
bility can be realized by improvements in cycle
efficiency. Increases in turbine inlet temperature
and increased pressure ratio result in higher cycle
efficiency and reduction in specific fuel consump-
tion.

The impact of higher cyclic efficiency and
future requirements with respect to combustors was
the topic of a forum held recently at the NASA
Lewis Research Center. The forum was conducted by
A. D. Little, Inc. and focused on the R & D effort
required to meet the critical need of combustors
for small gas-turbine engines in the 1980-90 time
frame.[1] Representatives of major small-engine
manufacturers and governmental users were invited
to participate in the forum in order to reach a
consensus regarding small combustor requirements.
The foremost area of concern was liner cooling.

Liner cooling is particularly critical in the
small gas-turbine engine due to the higher sur-
face-to-volume ratio of the combustor as compared
with large combustor systems. Higher cycle effi-
ciencies impose further demands on the cooling
problem. Less air is available for cooling due to
the increased fuel air ratio required to provide
higher turbine inlet temperatures. At the same
time the heat sink capability of the air has been
decreased because of higher combustor inlet temper-
ature resulting from increased pressure ratio.
Consequently, efficient use of coolant for liner
wall cooling is of utmost importance.

The liner cooling approach predominately used
in present day small combustors is splash film
cooling. The cooling air enters the liner through
a row of small diameter holes. The air jets impinge

on a cooling skirt, which then directs the flow so
as to form a film along the inside of the liner
wall. The total amount of cooling air required
depends on a number of factors; however, typical
values are in the range of 30 to 50 percent of the
combustor airflow.[2]

Improvements in film cooling effectiveness can
be achieved by using more efficient methods of air
scheduling and the heat sink available in the cool-
ing air as previously discussed.[3] Transpira-
tion cooling (continuous mass flux of coolant over
the surface) is one of the most effective methods
of liner wall cooling. Of the various concepts
using the porous wall principle Lamilloy is in the
most advanced stage of development and has shown
the potential of reducing the required amount of
cooling air by as much as 50 percent. The Lamilloy
concept features an electrochemically etched, mul-
tilayer, diffusion bonded structure.[4]

In this paper a reverse flow combustor using a
conventional splash film-cooled technique is com-
pared with a geometrically similar combustor with
Lamilloy liner walls. The reference film-cooled
combustor configuration has been previously re-
ported.[5] Documentation of performance,
emission index levels, and liner cooling effective-
ness over a range of simulated flight conditions of
a 16:1 compression ratio gas-turbine engine opera-
ting with Jet A fuel was obtained. Parametric
evaluation of the effect of increased combustor
loading is also included.

Apparatus

Test Facility

The test combustor was mounted in a closed-duct
facility (Fig. 1). Tests were conducted up to an
inlet-air pressure of 1600 kPa with the air indi-
rectly heated to about a temperature of 720 K. The
temperature of the air flowing out of the heat ex-
changer was automatically controlled by mixing the
heated air with varying amounts of cold bypassed
air. Airflow through the heat exchanger and bypass
flow system and the total pressure of the combustor
inlet airflow were regulated by remotely controlled
valves as indicated.

Combustor

The reverse flow combustor used in this inves-
tigation is a full-scale experimental NASA design.
A cross section and isometric views of the com-
bustor are shown in Fig. 2(b). The design stresses
versatility so that the interchanging of fuel in-
jectors and the modification or replacement of the
swirlers, faceplate, liner and turning sections can
be readily accomplished. The design liner isother-
mal pressure loss is 1.5 percent and the diffuser
dump loss is 0.24 percent. The airflow distribu-
tion and hole sizing in the liner are based on 36

primary and dilution holes. In this investigation two combustors with similar internal aerothermal design but with different liner wall cooling schemes were investigated.

Combustor Liners

Splash Film-Cooled. The design of the reference film-cooled wall construction combustor (Fig. 3(a)) was based, as far as feasible, on the procedure outlined in reference 6. The heat-flux balance is performed on an elemental length of the flame-tube wall, and conditions in the circumferential direction are assumed to be uniform. The combustor liner receives heat by convection (C_1) and radiation (R_1) from the hot gases within the combustor and loses heat by convection (C_2) to the incoming air between the liner and engine casing and by radiation (R_2) from the combustor liner to the casing; that is

$$R_1 + C_1 = C_2 + R_2 \tag{1}$$

The internal convection to the wall with film cooling is correlated to geometric and flow variables by

$$n = \frac{T_{ft} - T_{ad}}{T_{ft} - T_{ci}} \tag{2}$$

Where n is the film cooling effectiveness, T_{ft} is the temperature of the flame, T_{ad} is the the wall temperature and T_{ci} is the assumed to be the coolant inlet air temperature.

Although the original design did not include the effect of free stream turbulence on film cooling effectiveness, this effect was taken into consideration during the correlation of the experimental data by means of the following correlation:[7]

$$n_c = \frac{1}{1 + Cm \frac{x}{Ms}} \tag{3}$$

where C_m is the turbulent mixing coefficient, x is the distance downstream of the slot, M is the the mass flux ratio $\rho_s U_s / \rho_h U_h$, and s is the equivalent slot height.

A summary of the air distribution for combustion and coolant air is shown (see Table 1). The coolant flow requires 32.5 percent of the total mass flow. The percentage of coolant air is shown for the outer and inner walls (Fig. 4). The air entry locations are ratioed to the total length of the outer liner from the fuel injector faceplate to the turbine stator location. The coolant for the combustion zone and the reverse turn is also indicated.

Transpiration. Lamilloy was used to simulate transpiration cooling. A Lamilloy is a commercial product composed of an electrochemically etched channel structure in multilayers which is diffusion-bonded forming a sheet. The potential of a true transpiration surface is approached as discussed by Nealy and Reider.[4] An isometric sketch of the material is shown schematically in Fig. 3(b).

The Lamilloy combustor was fabricated under government contract to be similar to the reverse flow film-cooled geometry and to interface with the existing NASA test facility. The basic design con-

ditions were for a peak combustor operating pressure of 16 atmospheres, 717 K inlet temperature, and 1390 K exit with hot streaks up to 1922 K. The design pressure drop across the liner was 1.5 percent. The design of the Lamilloy reverse flow annular combustor follows the general flow charts of Ref. 8 (as shown in Fig. 5). Required local cooling flows were determined and matched to Lamilloy flow characteristics. The Lamilloy sections of the combustor were fabricated using Inconel IN 601.

The ideal blowing rate, G_c (coolant flow per unit solid wall area), was derived by making a simple heat balance on an element of the combustor; that is

Radiation Load + Convective load =
Cooling-air heat pick-up   (4)

The thermal effectiveness used in this analysis was defined as

$$n_t = \frac{T_{co} - T_{ci}}{T_{ws} - T_{ci}} \tag{5}$$

where T_{co} is coolant outlet temperature, T_{ci} is coolant inlet temperature, and T_{ws} is flameside wall surface temperature.

The cooling effectiveness of the Lamilloy wall is reflected in the thermal effectiveness, while the insulating of the film effect is taken into account by reducing the gas-to-wall heat transfer coefficient. In this analysis, the thermal effectiveness was taken to be 0.5, which is an experimentally determined value for the range of design blowing rates used in this application. A reduction of the gas-to-wall heat transfer coefficient was not taken due to a lack of data relating this effect for Lamilloy. Instead a relatively straightforward calculation was used to determine the average Nusselt number for turbulent flow over a flat plate, that is,

$$Nu_x = 0.037 \ (Re_x)^{0.8} \ (Pr)^{1/3} \tag{6}$$

and the gas-to-wall heat transfer coefficient calculation, h, obtained from $Nu_x = hx/k$, where k is the thermal conductivity and x is a characteristic length.

The flow characteristics of the Lamilloy are characterized by a coefficient of discharge (C_d) defined as

$$C_d = \frac{Gc \sqrt{Tc}}{\bar{P}} \left[\frac{\Delta P(2g)}{\bar{P}(R)}\right]^{-1/2} \tag{7}$$

where T_c is the average coolant temperature, $\bar{P}$ is the average pressure in Lamilloy wall, ΔP is the static pressure drop across the Lamilloy wall.

In the final design equation (7) was used to determine the actual flowing rate once the specific Lamilloy configurations were selected.

For this application three Lamilloy configurations were selected with C_d's of 0.005, 0.002, and 0.004 for the liner walls. (See Fig. 6.) The total Lamilloy wall cooling flow in this design is 25.6 percent as compared with 32.5 percent for the reference film-cooled combustor. The mass flow distribution is shown in Fig. 4 for the comparison with the film-cooled design. If the optimum con-

2

figirations were used to match the wall cooling requirements, the ideal mass coolant was calculated to be 20.6 percent.

Instrumentation

The liner thermocouple selection was based on thermal paint indications and liner wall locations representative of primary, secondary, and dilution regions. The splash film-cooled liner was instrumented with six Chromel-Alumel thermocouples imbedded in the 'cold' side of the liner and located as shown in Fig. 6.

The Lamilloy combustor was coated with a proprietary thermal paint, fired at NASA Lewis, and returned to the contractor for interpretation. A photograph of the fired Lamilloy combustor is shown in Fig. 7. The thermocouples were located (see Fig. 6) so as to include the hottest location as well as average region on the combustor inner and outer liner walls. Twelve Chromel-Alumel couples were mounted on the cold side of the Lamilloy to monitor liner temperature.

The combustor instrumentation stations are shown in Fig. 8. Five total pressure probes, two static pressure taps, and four Chromel-Alumel thermocouples are located at station 2 to measure the inlet temperature and pressure. At station 3 a series of 18 total pressure probes are installed to determine the inlet-air profile and to determine the extent of any flow disturbance behind the struts which support the centerbody diffuser. At station 4 six pitot-static probes are positioned in the cold-air passages between the combustor liner and combustor housing to determine passage velocity and distribution. At station 5 outlet temperature and pressure measurements are obtained by means of a rotating probe. The probe contains three rakes spaced 120° apart, a five-position radial rake containing Pt - Pt-13-percent Rd thermocouples, a five-position total pressure rake, and a water-cooled gas sampling rake. A 360° travel is used with increments as low as 1°. Ten degree increments were used for this program.

PROCEDURE

Test Conditions

The experimental reverse flow combustor was operated at test conditions based on a gas-turbine engine cycle with a compressor pressure ratio of 16. A tabulation of the test conditions simulated in this study is given in Table 2.

Data were obtained at combustor inlet conditions simulating sea level take-off (SLTO), cruise, and idle. Simulated flight data were obtained at a fuel-air ratio of approximately 0.024, low power at 0.020, and idle at 0.008. The simulated combustor test conditions are based on a reference velocity of 5.49 meters per second (m/s). The reference velocity quoted is based on undirectional total mass flow and the maximum cross-sectional area of the housing prior to the reverse turn (Fig. 2(a)). Parametric variations in velocity of 5.49, 7.32, and 9.14 m/s were also obtained during the experimental testing over a range of fuel-air ratios up to approximately 0.024. The test program was conducted using Jet A fuel with 18 simplex pressure-atomizing fuel injectors with a flow number of 4.8.

Emission Measurements

Exhaust gas samples were obtained according to recommended procedures.[9,10] Exhaust gases were withdrawn through the water cooled rotating probe mounted approximately in the stator plane and in the center of the exhaust duct at station 5 (Fig. 8). The gas sample temperature was held at approximately 423 K in the electrically heated sampling line. Most of the gas sample entered the analyzer oven, while the excess flow was bypassed to the exhaust system. To prevent fuel accumulation in the sample line, a nitrogen purge was used just before and during combustor ignition.

After passing through the analyzer oven, the gas sample was divided into three parts, and each part was analyzed. Concentrations of oxides of nitrogen, carbon monoxide and carbon dioxide, and hydrocarbons were measured by the chemiluminescence, nondispersed-infrared, and flame-ionization methods, respectively. Details of the gas analysis system are presented in Ref. 5. The combustion efficiency data presented in this paper were based on stoichiometry determined by gas analysis.

RESULTS AND DISCUSSION

Two reverse flow combustors - one with conventional splash film-cooled walls and the other with a simulated transpiration cooled wall technique (Lamilloy) - were operated at test conditions typical of a 16:1 pressure ratio turbine engine. Combustion efficiency, emissions, outlet temperature distribution, and liner temperature data are compared for simulated flight conditions and a parametric variation of increased combustor loading.

Performance

Combustion Efficiency. The combustion efficiency data are presented in Fig. 9 for the two combustor wall configurations. At simulated flight conditions efficiency levels near 100 percent were indicated for the reference film-cooled combustor. Parameteric effects of combustion efficiency at reduced power are also indicated (Fig. 9) (i.e., pressure levels of 850 kPa or lower at a constant fuel air ratio of 0.02). At reduced power the combustion efficiency remained near 100 percent but started to drop off at pressure levels below 600 kPa. The reference configuration was tested using 18 simplex fuel injectors. Reducing the number of fuel injection points by blocking off every other fuel injector improved the efficiency at low power. As previously reported the effect of combustion efficiency in the reference film-cooled combustor was dependent on fuel atomization.[5] At low flows the fuel spray deteriorates with simplex pressure atomizing injectors. By reducing the number of fuel injectors an improvement in spray characteristics results and efficiency improves.

With the Lamilloy combustor using the basic 18 fuel injector configuration efficiency levels near 100 percent were obtained at simulated flight conditions; however, as power levels were reduced below 650 kPa combustion became unstable and blowout was subsequently experienced. Reducing the number of fuel injectors improved low-power performance and blowout characteristics, and results similar to the reference film-cooled configuration were obtained.

While slight differences in combustion efficiency were observed the combustion characteristics were similar except that the Lamilloy configuration was less stable at reduced fuel flows with 18 fuel injectors. This may in part be due to the influence of the coolant film in triggering a mini-recirculation zone to provide a favorable flame seat in the film-cooled design. The design airflow entering into the primary reaction zone was within 0.16 percent for each of the two designs (i.e., 26.63 percent for the film-cooled and 26.79 percent for the Lamilloy). The measured total pressure drop between the two configurations was similar; consequently, since air entry placement was similar, the basic internal aerodynamics and recirculation patterns would be expected to be similar. It was considered that the design transfer from the film-cooled configuration to Lamilloy was successfully accomplished.

Emissions. Even though it is not anticipated that emission standards will be established in the near future for small gas turbines in the under 6000-lb thrust class, emission levels are presented in this paper for comparison with the reference design. Emission index was less than 1 for unburned hydrocarbons (uHC) and less than 2 for carbon monoxide (CO) at simulated flight conditions. At low power uHC and CO emission levels increased in accordance with the loss in combustion efficiency as previously discussed. The uHC and CO emission levels were similar for the film-cooled and Lamilloy configurations.

The oxides of nitrogen (NO_x) emission levels are presented in Fig. 10 for inlet conditions representative of sea level take-off and a range of fuel-air ratios up to full power requirements. As shown the film-cooled liner produced an emission index of NO_x significantly more than the Lamilloy (i.e., emission index of 19.2 as compared with 12.2 gm/kg at SLTO).

The marked decrease of NO_x emission with the Lamilloy configuration is believed to be due to improvements in fuel-air uniformity as a result of better mixing. The factors which contribute to improved mixing in the Lamilloy configuration are due to minimum interaction of the air admission jets with the coolant and a resultant more vigorous internal aerodynamics.

The transfer of the basic design to Lamilloy involved a number of design compromises in order to maintain equivalent air-entry momentum ratio, hole size, and penetration depth. Film-cooling introduces a longitudinal flow field which must be re-established along the length of the combustor; whereas, the Lamilloy construction simulates a transpiration surface to form a protective film on the liner wall. The required design changes to establish the transpiration film result in less interference with primary and secondary air penetrations and hence, reduce perturbations of the internal aerodynamic flows.

It has been previously noted that fuel distribution markedly affected NO_x formation in the reference film-cooled configuration. Fuel distribution is primarily associated with the Sauter Mean Diameter (SMD) of the droplets, spray angle, and spatial mass distribution. In Ref. 11, it was shown that the NO_x level could be reduced from 19 to 13.5 gm/kg by changing the fuel injector type. The SMD was reduced from 100 to 75 μm and the spray angle increased from 75 to 90°. A reduction in SMD would not only improve vaporization due to increased surface area but also the droplet would have less drag, thereby more readily following the

internal aerodynamics. The increased spray angle would improve dispersion. These factors are conducive to improve mixing. Conversely, if the aerodynamics are more vigorous and the fuel spray similar, a decrease in NO_x would also be anticipated to occur.

In view of the sensitivity of NO_x formation to fuel and air distribution it appears that the low NO_x values obtained with the Lamilloy combustor are attributed to improvement in air introduction and mixing.

An additional source of NO_x formation may also have been minimized in the Lamilloy configuration by eliminating burning in the wake of coolant slots. The liner walls in a small combustor are of necessity rather close together and fuel penetration to the wall has been observed.

In the film-cooled configuration a weak recirculation exists at the slot which could provide the required air and the required stabilization for combustion to occur. If the mixture strength is within flammability limits, excessive NO_x production could result. Burning in the wake of film cooling slots has been observed previously. In the Lamilloy configuration such a condition cannot be readily established.

Outlet Temperature Distribution. The outlet temperature distribution as shown by pattern factor is presented in Fig. 11 at the simulated sea level take-off condition. The pattern factor is relatively uniform over a wide range of fuel-air ratios with a value of about 0.31 for the film-cooled liner and 0.15 for the Lamilloy. The improvement in pattern factor with Lamilloy is attributed to minimum mixing of the transpiration layer with the combustion gas.

The average radial profile of temperature distribution at the turbine position for simulated take-off is shown in Fig. 12. Included for reference is a typical profile based on consideration of fatigue, creep, and erosion of the turbine blades. As expected the combustor with Lamilloy liners produced the best average outlet temperature profile because of minimum interference of the coolant film at the wall. It should be noted that no attempt was made in this study to tailor the hot gas profile for a specific distribution.

Parametric Variation of Reference Velocity

The effect of increasing the mass flow for a given inlet pressure and temperature in the reverse flow combustor was investigated to determine the effect on performance factors. Nominal mass flow increases of 33 and 66 percent were tested at simulated cruise and sea level take-off. An increase in mass flow at the simulated test conditions is directly proportional to reference velocity.

The combustion efficiency obtained with the splash film-cooled and Lamilloy liner configurations was not appreciably affected by an increase in reference velocity. It remained at approximately 100 percent.

Emission levels of the oxides of nitrogen are shown in Fig. 13. The decrease in NO_x with increase in reference velocity (from 12.2 gm/kg to 10.5 gm/kg at a 66 percent increase in reference velocity with Lamilloy) was similar for each of the liner configurations. The decrease in NO_x is attributed to improved atomization and mixing as a result of the increased pressure drop of the air-stream, and due to decreased residence time.

Outlet temperature distribution as indicated by pattern factor degenerated as the reference veloc-

ity increased (Fig. 14). It should be noted that the simulated cruise condition was selected for comparison because the high fuel flows required for the sea level take-off simulation could not be achieved with only one fuel injector Flow Number value. There was an improvement in pattern factor of about 50 percent with the Lamilloy configuration at the cruise condition as compared with the reference film-cooled combustor (0.13 as compared with 0.25 at 5.5 m/s and 0.18 as compared with 0.35 at 9.1 m/s). Both combustor liners responded in a similar manner to increased loading as reflected by reference velocity.

Liner Temperature

The effect of combustor operating conditions and increased loading on liner cooling effectiveness is given for the film-cooled and Lamilloy liner walls (Fig. 15). For comparative purposes the cooling effectiveness is defined as

$$E_c = \frac{T_{ft} - T_{ad}}{T_{ad} - T_{ci}} \qquad (8)$$

where T_{ad} is the thermocouple measurement on the cold side of the combustor wall, T_{ft} is the calculated flame temperature, and T_{ci} is the measured inlet air temperature.

As the combustor pressure or mass loading increased at a constant fuel-air ratio the liner cooling improved. The panel selected for comparison is the inner wall prior to the turn. In general this is one of the most difficult areas to cool due to depletion of the mass flow in the annular passage. The film-cooled liner used 1.44 percent of the total flow to cool this panel; whereas, in the Lamilloy configuration the equivalent flow was 0.7 percent. Even though approximately 50 percent less air was required for the Lamilloy the cooling effectiveness was similar. At increased reference velocity (mass loading) the cooling effectiveness of Lamilloy increased more than the film-cooled design. This can probably be attributed to the higher pressure drop across the liner as well as the increased heat dissipation to the various heat sinks.

It should be noted that the Lamilloy cooling effectiveness was calculated from thermocouple indications on the cold wall. Thermocouple measurement yielded a range from 950 to 1060 K for the cold side, and calculations indicated that a maximum of 1132 K would be predicted for the flame side, both within the maximum design limit of 1200 K.

In the transition section the cooling effectiveness was similar between the two liner configurations. The film-cooled design, however, used 15.8 percent of the total air for cooling while 7.85 percent was used for the Lamilloy (about 50 percent less coolant). The predicted cooling effectiveness for Lamilloy as compared with film cooling is given (see Fig. 16). These data for the combustor and turn section are both within the expected improvement in coolant effectiveness. In the case investigated this design used about 50 percent less coolant for the Lamilloy than the film-cooled design comparison goals.

It was previously indicated that the liner walls in the Lamilloy were purposely overcooled in order to balance out the internal aerodynamics and simplify design by using 'stock' design geometries

for the internal Lamilloy flow passages. As a result 25 percent of the air was used for coolant whereas 20 percent was considered sufficient. This compares with 33 percent considered for 'rule-of-thumb' type of calculation considering the engine pressure ratio simulation.[2]

In the film-cooled design 32.5 percent of the air was used for wall coolant. Experimental testing indicated that the film-cooled liner was also overcooled in the reverse turn. In this case, the film-cooled design used approximately 50 percent more coolant than Lamilloy. It is probable that the excess coolant air detached from the liner wall in the film-cooled design and migrated toward the inner turn. The behavior of a diluent in an accelerating flow field in the turning section of a reverse flow combustor has shown that a cold jet from the outer wall will migrate toward the inner wall.[12] In addition, injection from an inner wall will also produce a jet which tends to follow the inner wall. In the case of the Lamilloy design, the transpiration film was more effectively attached to the outer wall and being a smaller percentage of the flow resulted in the improved outlet radial temperature distribution as previously shown (see Fig. 12). Although it was apparent in the experimental evaluation of the reference design that the transition section was excessively cooled, it was not within the scope of this program to modify the wall cooling to better schedule and optimize the design. In this case it was estimated that both the film-cooled and Lamilloy were overcooled especially on the outer turn of the transition section. The behavior of an accelerating flow field in the turn can partly explain the experimental results.[12] As a consequence the convective heat transfer on the flame side (i.e., C_2 in eqs. (1) and (4)) should probably be reevaluated to consider a less turbulent environment.

One of the approaches used to correlate liner temperature levels by means of cooling effectiveness for a film-cooled liner is to consider the film mass flow rate and hot stream turbulence level.[7] Using the experimental value of liner temperature and assuming that the temperature of the film at any downstream location is equal to the wall surface temperature, a value of the turbulent mixing coefficient (C_m) was obtained using equation (3). The flame side Mach number along the length of the combustor was calculated assuming one-dimensional premixed combustion gases. In Fig. 17, the calculated C_m for a given Mach number is shown for the film-cooled combustor liner. A value of C_m of 0.04 is shown to correlate the data in the primary zone and 0.008 at the exhaust. Data from a series of tests with the film-cooled liner indicate that there is also a slight effect of combustor film Reynolds number on C_m.

Previous data have indicated that a coefficient of 0.15 was experienced for the combustor used to develop the correlation. The small combustor and particularly the reverse flow combustor tend to operate with lower reference velocities than most contemporary larger combustors. The lower overall reference velocity is in keeping with the low turbulence level.

At the exhaust the reference Mach number has increased and the C_m has reduced. The flow can be represented by a series of streamlines with minimum mixing[12]. As a consequence the turbulent mixing coefficient is reduced due to the smoothing out of the flow field. These results also indicate that the effective film heat transfer coefficient should be somewhat more conservative in

5

the transition section than would be normally considered. It should be noted that in this study for the design of the reverse flow reference combustor the heat transfer coefficient was evaluated by assuming the boundary layer to be turbulent over the whole length.

CONCLUSIONS

1. The transfer of a film-cooled reverse flow combustor design to a transpiration (Lamilloy) configuration was successfully accomplished by using existing design procedures. Experimental measurements over a range of simulated turbojet engine operating conditions indicated similar performance of combustion efficiency and pressure loss levels.

2. The Lamilloy combustor required 50 percent less coolant in critical areas as compared with the equivalent panels in the film-cooled configuration.

3. The internal transpiration film resulted in an improvement not only with respect to coolant management and liner temperature level but also in pattern factor, average circumferential radial outlet temperature profile, and reduction in NO_x emission index.

4. It was shown that existing design correlations could be improved in the reverse flow combustor application by considering a less turbulent flow than for larger combustors.

REFERENCES

1. Demetri, E. P., Topping, R. F., and Wilson, R. P., Jr., "Study of Research and Development Requirements of Small Gas-Turbine Combustors," Arthur D. Little, Inc., Cambridge, MA., ADL-83381-2, Jan. 1980. (NASA CR-159796).

2. "The Design and Performance Analysis of Gas-Turbine Combustion Chambers, Vol. 1, Theory and Practice of Design.," Northern Research and Engineering Corporation, NREC Rept. No. 1082-1, 1964.

3. Colladay, Raymond S., "Analysis and Comparison of Wall Cooling Schemes for Advanced Gas Turbine Applications," NASA TN D-6633, Feb. 1972.

4. Nealy, D. A., and Reider, S. B., "Evaluation of Laminated Porous Wall Materials for Combustor Liner Cooling," ASME Paper 79-GT-100, Mar. 1979.

5. Norgren, C. T., and Riddlebaugh, S. M., "Effect of Fuel Injector Type on Performance and Emissions of Reverse-Flow Combustor," NASA TP-1945, Dec. 1981.

6. "Computer Program for the Analysis of Annular Combustors, Vol. 1.," Northern Research and Engineering Corporation, Report 1111-1, Jan. 1968. (NASA CR-72374.)

7. Juhasz, A. J., and Marek, C. J., "Combustor Liner Film Cooling in the Presence of High Free-Stream Turbulence," NASA TN D-6360, July 1971.

8. Petraits, J. J., "Design and Fabrication of Lamilloy Reverse Flow Combustor Liners," Detroit Diesel Allison, EDR-9803, Apr. 1979. (NASA Contract NAS3-21222.)

9. "Control of Air Pollution from Aircraft and Aircraft Engines - Emission Standards and Test Procedures for Aircraft," Federal Register, Vol. 38, No. 136, Pt. 2, Tues., July 17, 1973, pp. 19088-19103.

10. "Procedures for the Continuous Sampling and Measurement of Gaseous Emissions from Aircraft Turbine Engines," SAE Aerospace Recommended Practice 1256, Oct. 1971.

11. Norgren C. T., and Riddlebaugh, S. M., "Small Gas-Turbine Combustor Study - Fuel Injector Evaluation," AIAA Paper 81-1387, July 1981. (NASA TM-82641.)

12. Riddlebaugh, S. M., Lipshitz, A., and Greber, I., "Dilution Jet Behavior in the Turn Section of a Reverse Flow Combustor," AIAA Paper 82-0192, Jan. 1982. (NASA TM 82776.)

Table 1. Liner Airflow Distribution

Air entry	Type of entry	Mass flow, percent of total	Comments
Faceplate	Swirler	24.8	2.54 cm from firewall, 36 holes in outer wall, and 36 holes in inner wall
Primary	Primary holes	18.6	5.72 cm from firewall, 36 holes in outer wall, and 36 holes in inner wall
Dilution	Dilution holes	24.1	---
Concentric around fuel injector	Annulus	3.2	---
Liner cooling	Film cooling	13.2	---
Outer 180°	Film cooling	13.1	---
Inner 180°	Film cooling	3.0	---

Table 2. Reverse-flow-combustor test conditions

Test condition	Total airflow		Inlet pressure		Inlet temperature		Reference velocity		Simulated compressor pressure ratio	Comments
	kg/sec	lb/sec	kPA	psia	K	°F	m/s	ft/sec		
A	2.27	5	1014	147	686	775	5.5	18	10	High-altitude cruise
B	3.05	6.71	1358	197	703	805	5.5	18	13.4	Low-altitude cruise
C	3.63	8	1620	235	717	830	5.5	18	16	Sea level take-off (SLTD)
D	1.23	2.70	405	58.5	474	394	5.2	16.9	4	Idle: f/a = 0.008
E	2.12	4.66	862	125	627	668	5.5	18	8.5	Simulated reduced power
F	1.83	4.02	689	100	581	585	---	--	6.8	
G	1.51	3.33	517	75	526	486	---	--	5.1	
H	1.23	2.70	414	60	474	394	---	--	4.1	
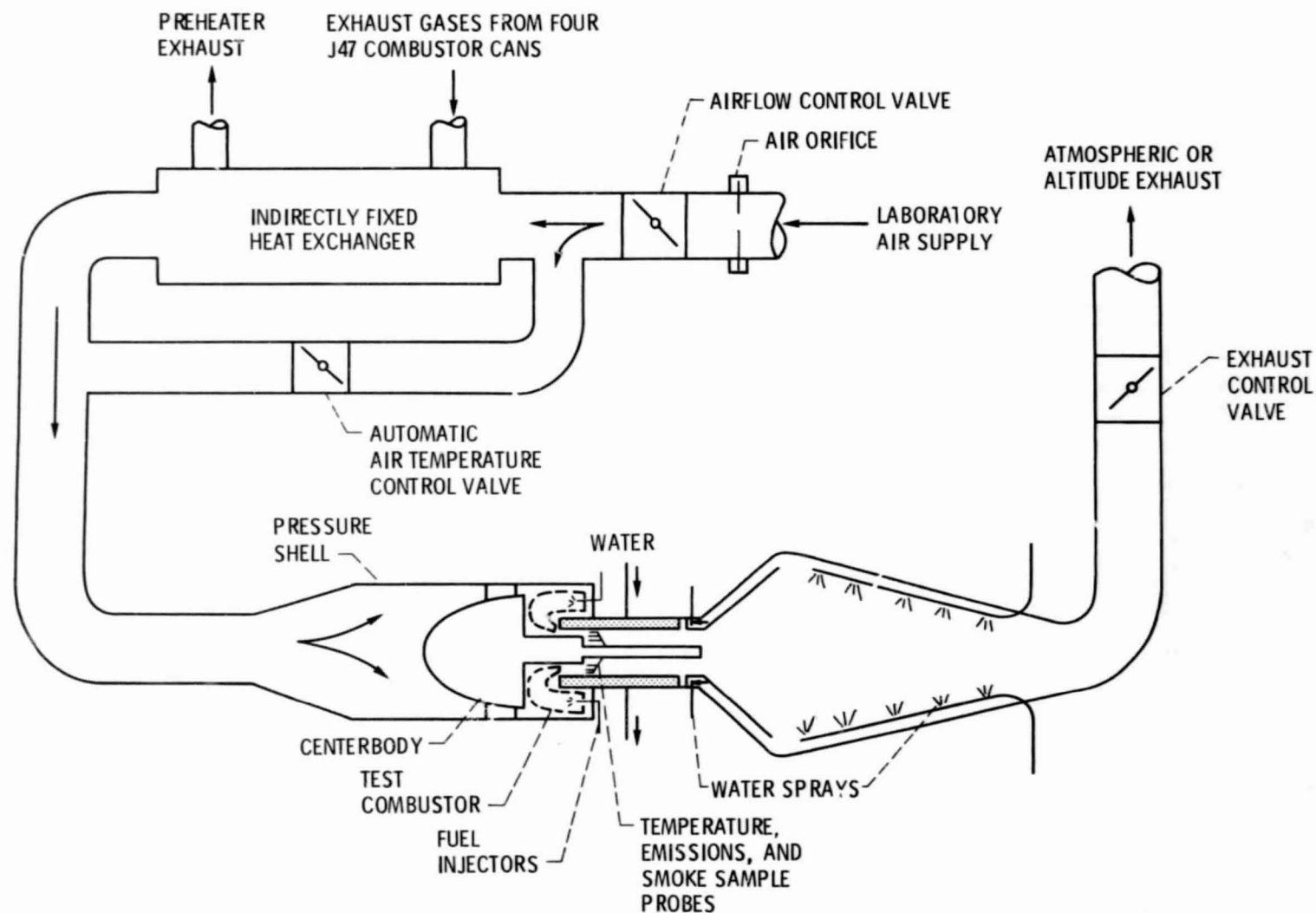
Figure 1. - Schematic of test facility.

(a)

INSTRUMENTATION STATION 3

21.5

○ LINER THERMOCOUPLE LOCATIONS

AIRFLOW →

FUEL INJECTOR

38.5 diam

40.64 diam

5.0

AIR SWIRLER

25.17 diam

REFERENCE AREA, 800 cm^2

1.8

→ EXHAUST

INSTRUMENTATION STATION 5
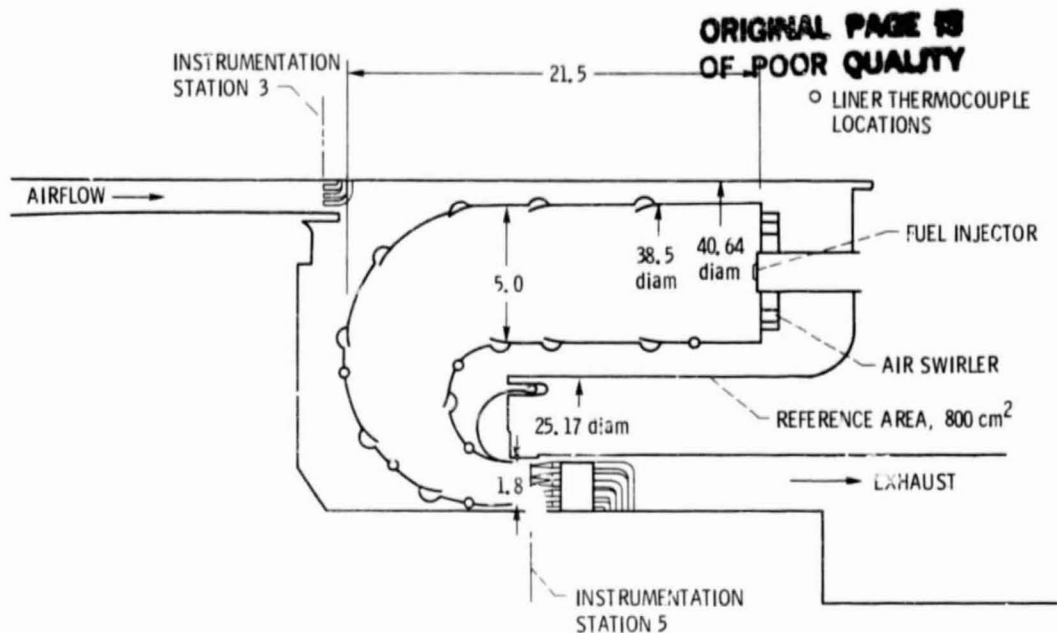
COMBUSTOR CENTERLINE
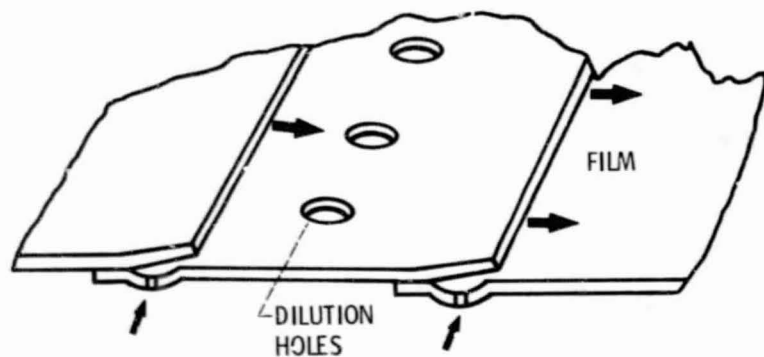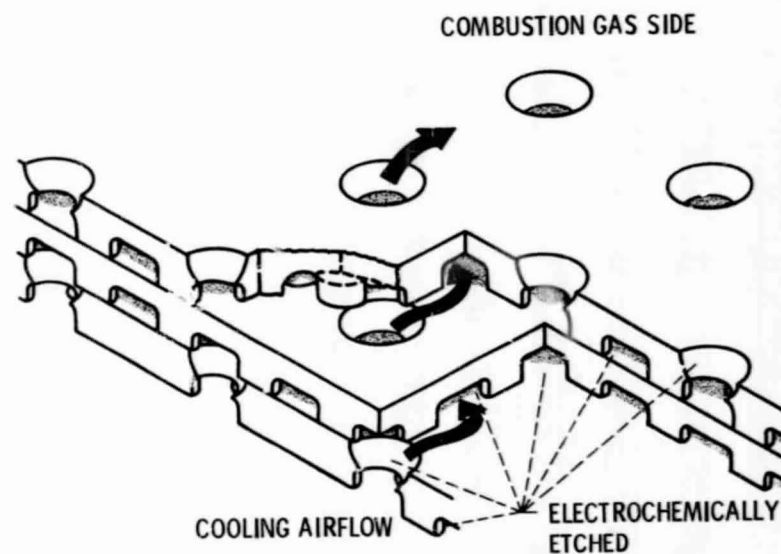
(b)

AIRFLOW

FUEL INJECTORS

REVERSE TURN

HOT EXHAUST

'CRITICAL' LINER PANEL
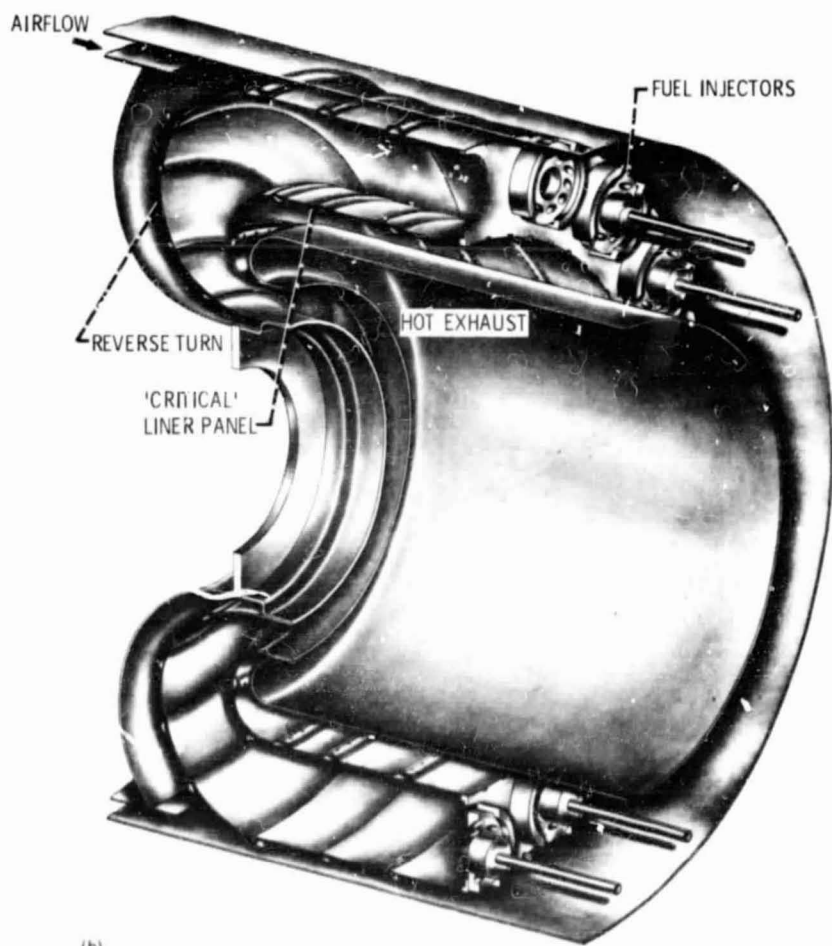
(a) Cross section.

(b) Isometric view.

Figure 2. - Reverse-flow combustor. (All dimensions are in centimeters.)

COMBUSTION GAS SIDE

FILM

DILUTION
HOLES

COOLING AIRFLOW

ELECTROCHEMICALLY
ETCHED

(a) FILM COOLED.

(b) LAMILLOY.

Figure 3. - Schematic of liner wall cooling configurations.
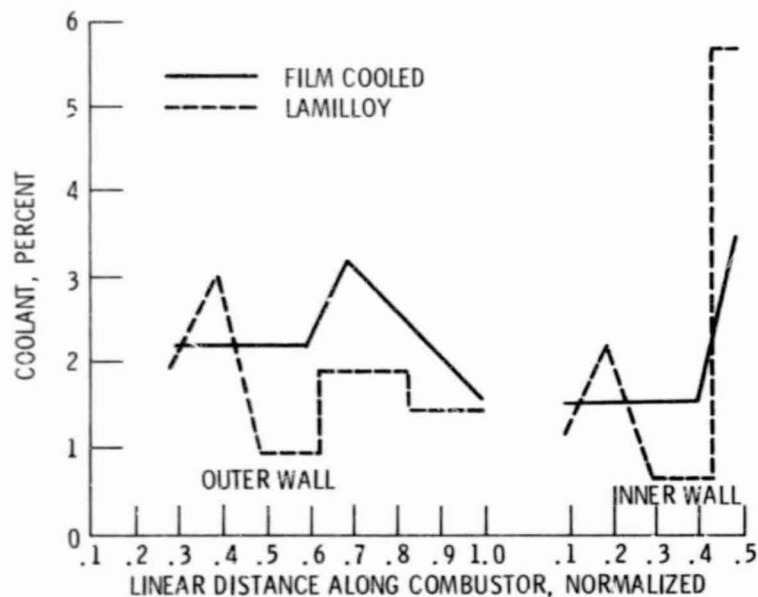
Figure 4. - Coolant mass flow distribution.

COMBUSTOR PRELIMINARY DESIGN
- OPERATING CONDITIONS, AIR DISTRIBUTION, $\frac{\Delta P}{P}$, MATERIAL SELECTION
- BUCKLING, AXIAL STRESS ANALYSIS
- LOCAL FLAME TEMPERATURES (AVERAGE & HOT STREAK)

HEAT TRANSFER ANALYSIS - DEFINE IDEAL WALL COOLING FLOW RATES FOR 1700F MAXIMUM WALL TEMPERATURE

LAMILLOY SELECTION TO MATCH CONFIGURATIONS TO IDEAL COOLING FLOW RATES

RECALCULATE COMBUSTOR AIRFLOW DISTRIBUTION, $\frac{\Delta P}{P}$, LOCAL f/a RATIOS AND FLAME TEMPERATURES (AVERAGE AND HOT STREAK)

HEAT TRANSFER ANALYSIS TO CALCULATE WALL TEMPERATURES

STRESS ANALYSIS OF FINAL CONFIGURATION WITH CALCULATED WALL TEMPERATURES AND TEMPERATURE DIFFERENTIALS

COMBUSTOR FINAL DESIGN

FABRICATION

Figure 5. - Lamilloy combustor design flow chart.
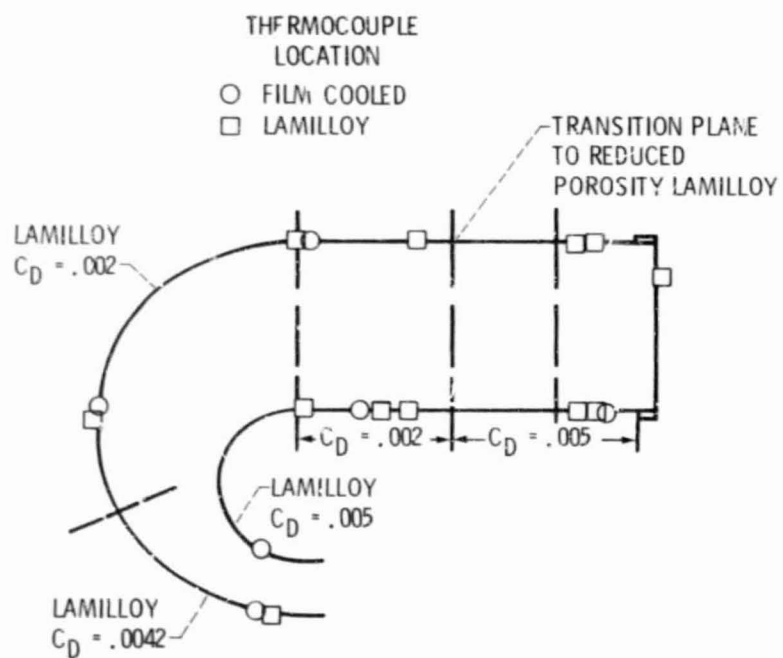
Figure 6. - Lamilloy identification for reverse flow annular combustor.
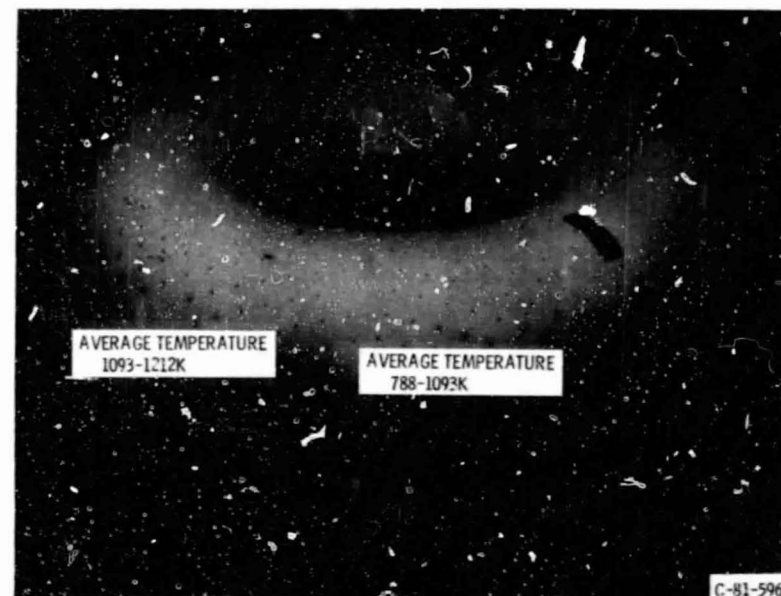
Figure 7. - Photograph of lamilloy combuster after firing.
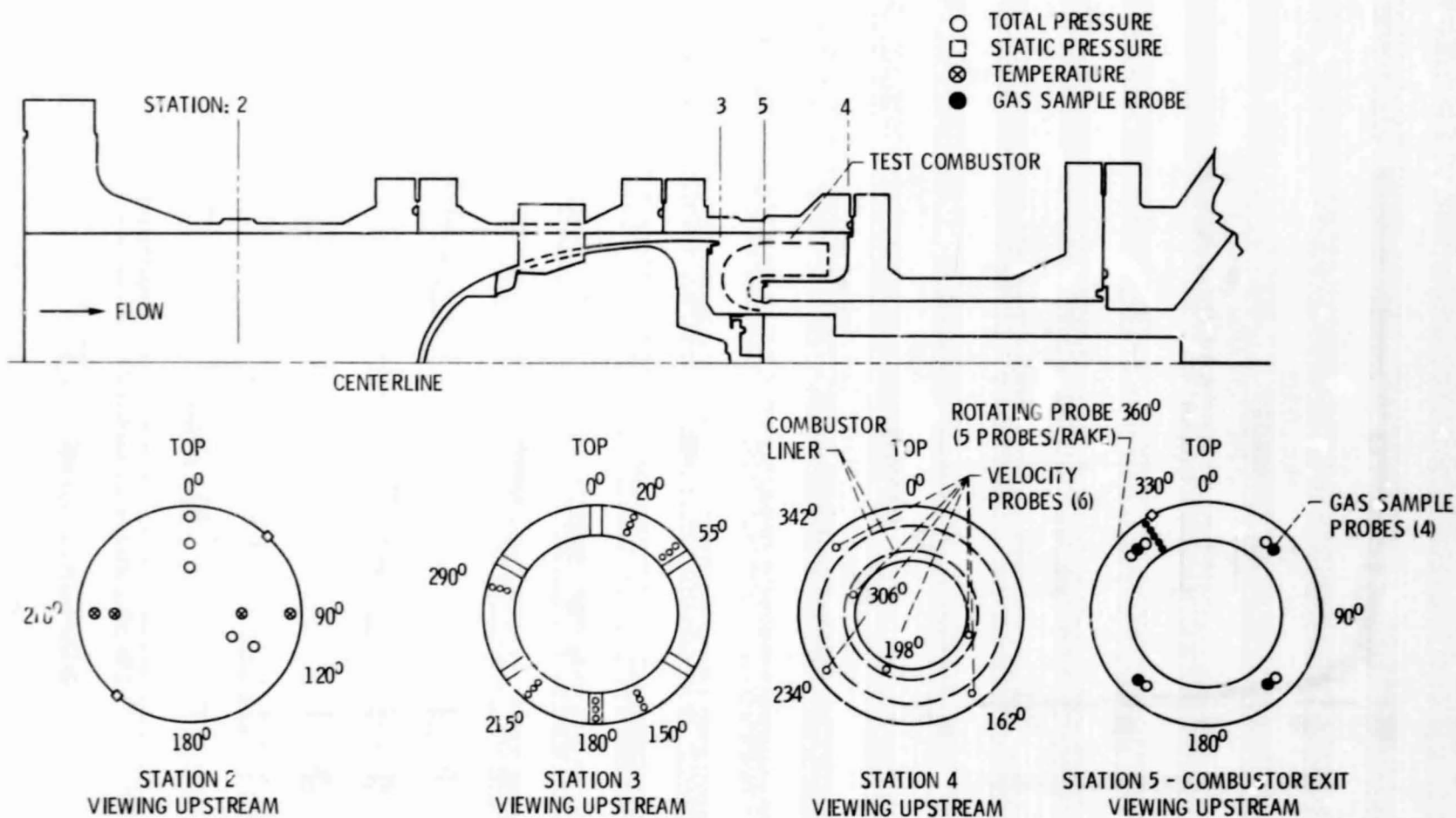
Figure 8. - Research instrumentation.
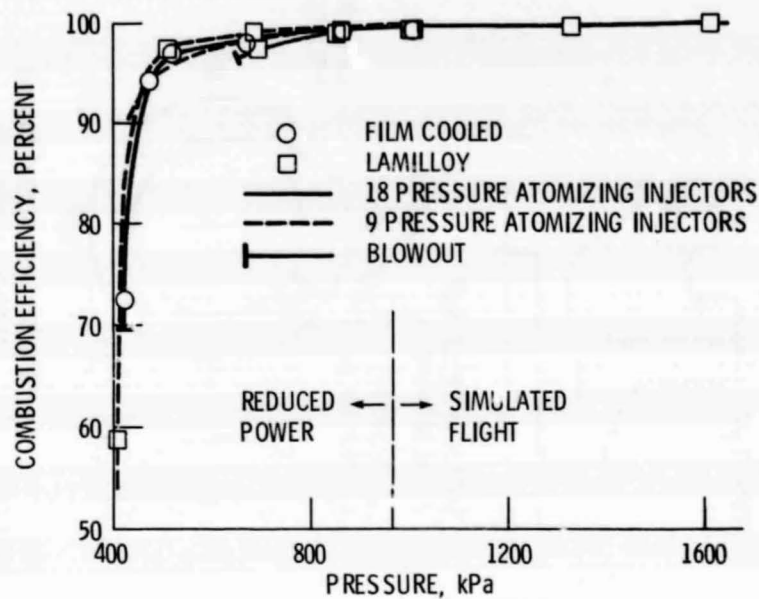
Figure 9. – Comparison of combustor efficiency with film cooled and Lamilloy combustors.
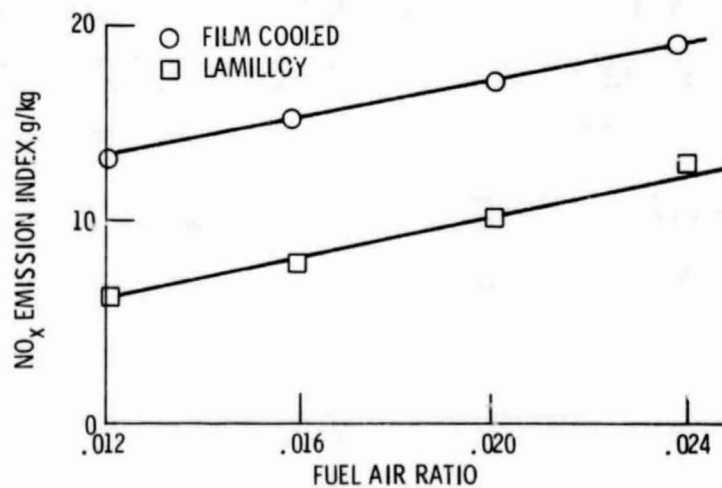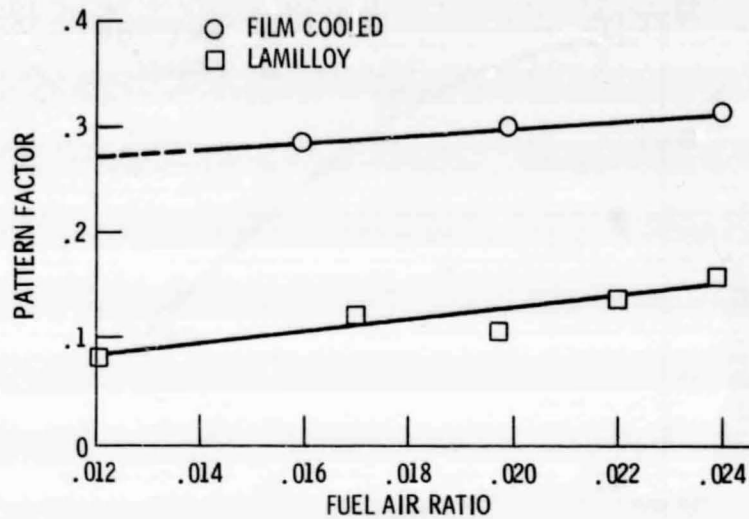

Figure 10. – Oxides of nitrogen emission comparison of film cooled and Lamilloy combustors over a range of fuel air ratios. (Combustor inlet typical of S.L.T.O. 16:1 pressure ratio turbojet engine.)
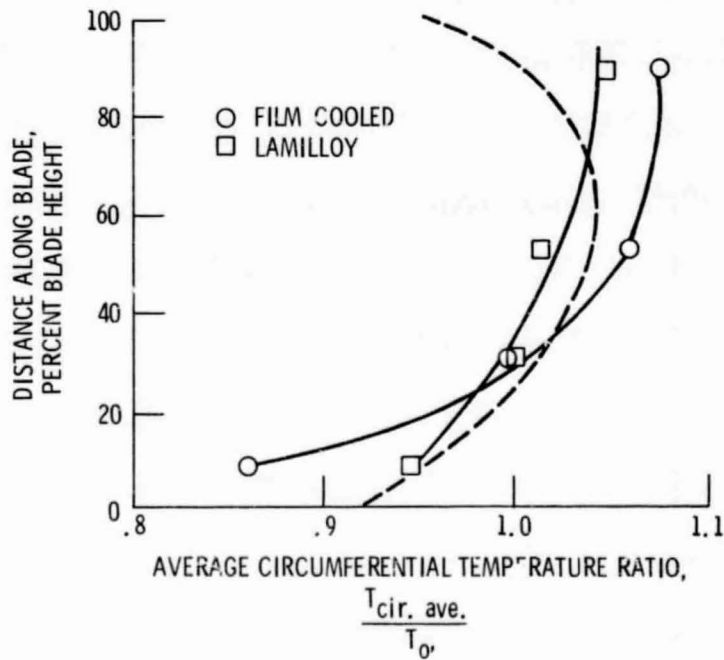
Figure 11. - Pattern factor comparison of film cooled and
Lamilloy combustors over a range of fuel air ratios.
(Combustor inlet typical of S.L.T.O. 16:1 pressure ratio
turbojet engine.)

Figure 12. - Comparison of radial temperature profiles at
discharge of Lamilloy and film cooled combustors.
(Combustor operation typical of S.L.T.O. conditions of
a 16:1 pressure ratio turbojet engine).
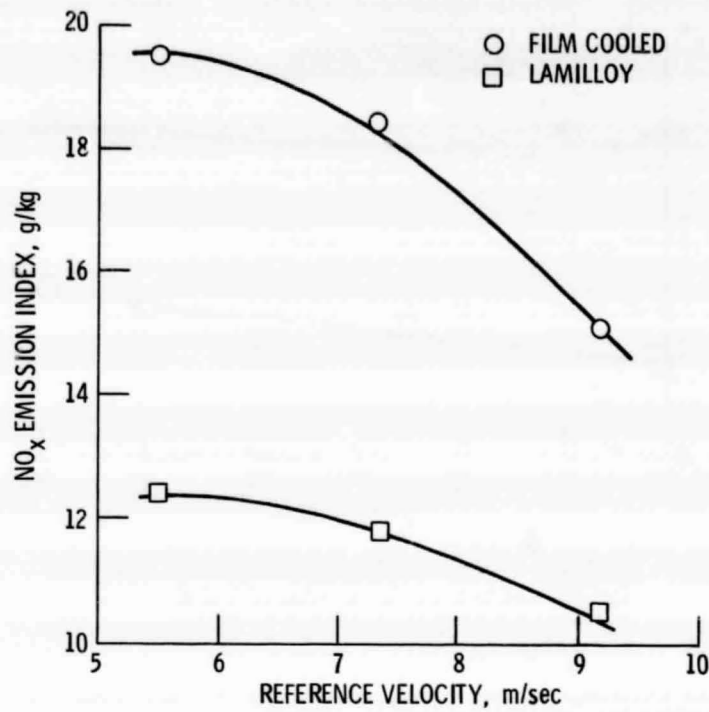
Figure 13. - Effect of parametric variation of reference
velocity on NO$_x$ emission for film cooled and Lamilloy
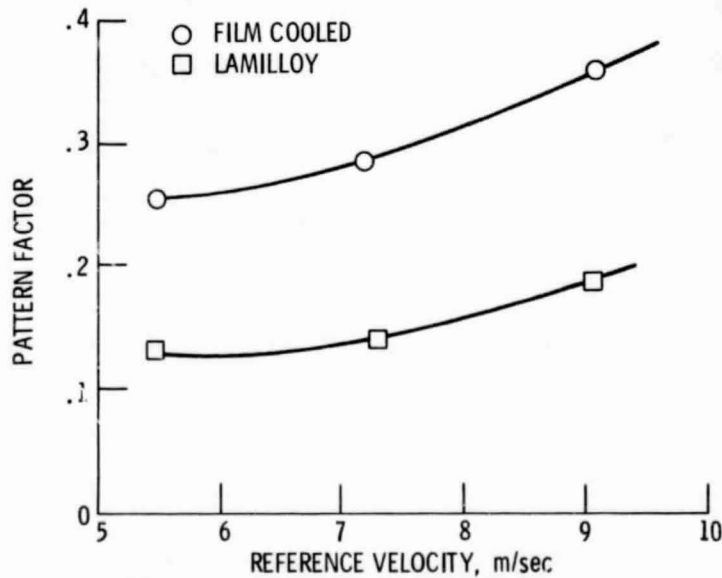combustors. (Simulated S.L.T.O. 16:1 pressure ratio
turbojet engine.)

Figure 14. - Effect of parametric variation of reference
velocity on pattern factor for film cooled and Lamilloy
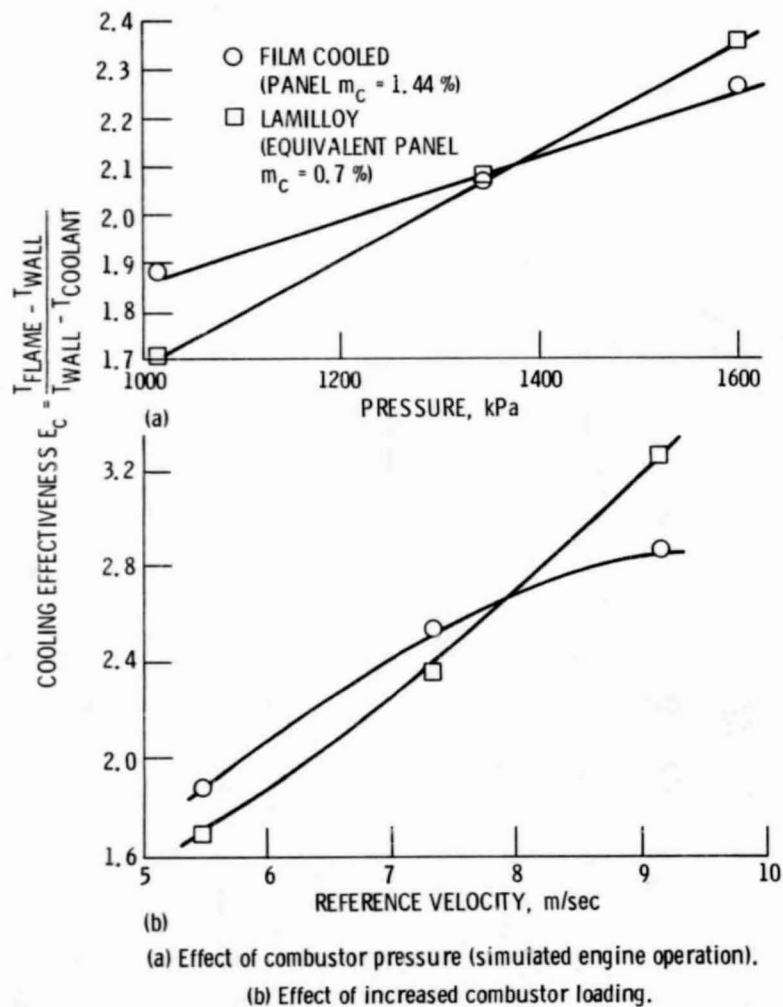combustors. (Simulated cruise 16:1 pressure ratio
turbojet engine.)

(a) Effect of combustor pressure (simulated engine operation).

(b) Effect of increased combustor loading.

Figure 15. - Comparison of cooling effectiveness for film cooled
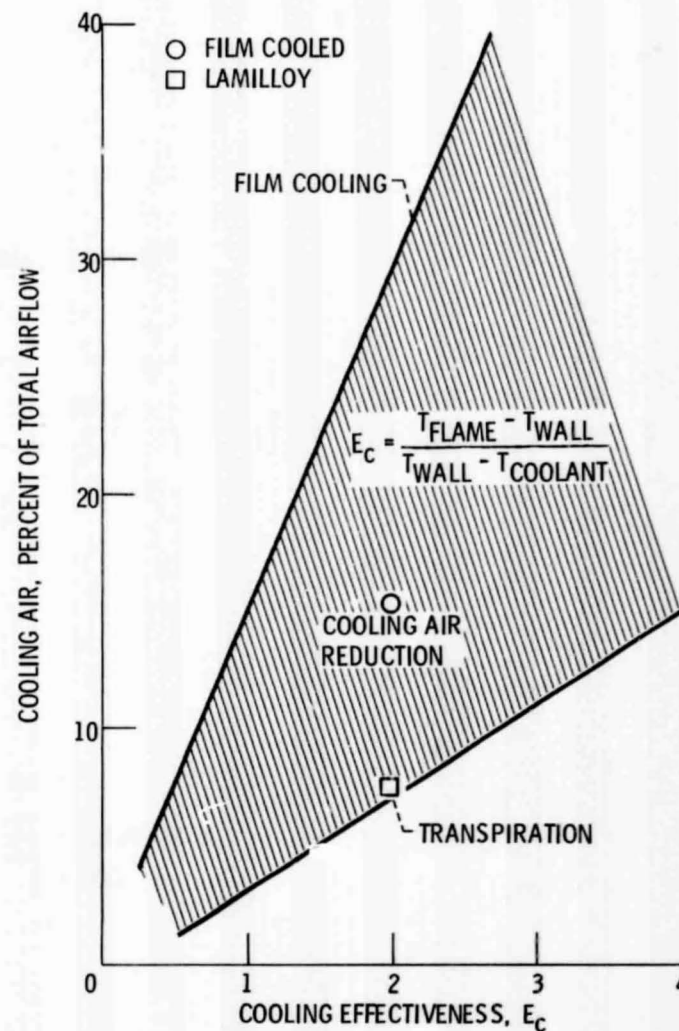and Lamilloy combustor liner at a nominal fuel air ratio of
0.024.

Figure 16. - Relative cooling performance of film cooled
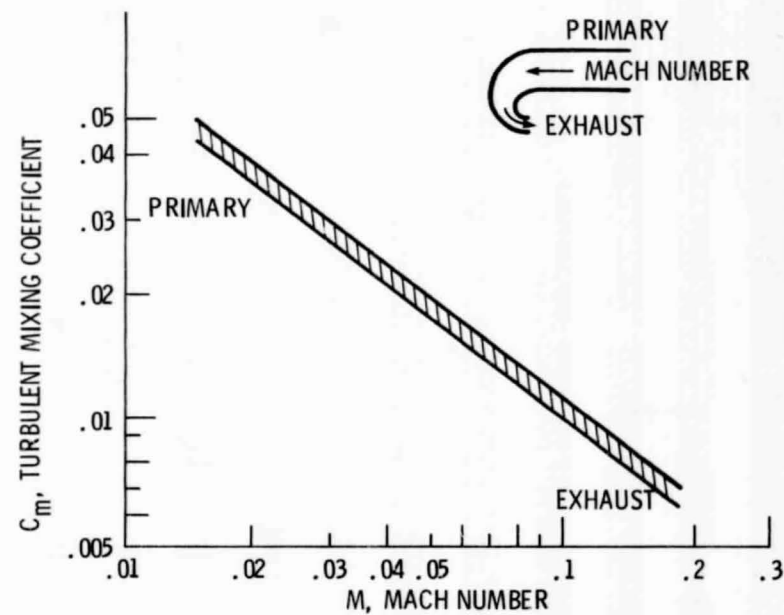and transpiration cooled combustors.

Figure 17. - Reverse flow combustor film cooling.